Distributed Feedback-Like Laser Emission in Photonic Crystal Waveguides on InP Substrate

Xavier Checoury, Philippe Boucaud, Jean-Michel Lourtioz, Frédéric Pommereau, C. Cuisin, E. Derouin, O. Drisse, L. Legouezigou, O. L. Legouezigou, François Lelarge, F. Poingt, Guang-Hua Duan, *Senior Member, IEEE*, S. Bonnefont, D. Mulin, J. Valentin, O. Gauthier-Lafaye, F. Lozes-Dupuy, and A. Talneau

***Abstract*—Lasing of triangular and square lattice photonic crystal, waveguides on InP substrate is investigated around the 1.5-μm wavelength by optical pumping. The lattice period of the fabricated structures is varied over a very large scale, thereby allowing a detailed exploration of the laser behaviors in the cases of micrometer width waveguides. A genuine distributed feedback (DFB) laser emission is observed in the gap for W2-3 waveguides in the ΓM direction of a triangular lattice. A different behavior is obtained for W3 waveguides in the ΓK direction of the same lattice as well as for W1 and W3 waveguides in the ΓX direction of a square lattice. The laser emission is found to occur at the Γ point of the Brillouin zone (wavevector $k = 0$) when the emission frequency is outside the gap. The DFB-like laser emission is intrinsically single mode in this case. Plane wave calculations show that the field distributions of the two DFB components are radically different. The emitting mode is well localized in the guide core while the non-lasing mode spreads over the whole crystal.**

***Index Terms*—Photonic crystal (PhC), plane wave method, semiconductor laser, waveguide.**

I. Introduction

PHOTONIC CRYSTALS (PhCs) appear as one of the possible ways toward the large-scale integration of photonic devices in telecommunication systems. They have recently been used for the fabrication of narrow ($\leq$ 1-μm wide) waveguide edge-emitting lasers [1], [2], which respectively consisted of one and three rows of missing holes (respectively, W1 and W3) in a perforated membrane. The laser emission was attributed to low-group-velocity guided modes located below the light cone leading to low-loss diffraction. Such a situation is indeed very favorable to high-gain laser modes. However, the membrane approach is penalized by the presence of heating effects and by a difficult implementation of electrical pumping. From this point of view, the so-called substrate approach classically based on multilayer waveguides appears to be better adapted to the large-scale integration of photonic devices. In contrast, the small refractive index difference between the guiding and cladding layers results in a weaker confinement of light in the vertical direction, and most likely, in higher losses than in the membrane approach. Experimental data are thus desirable for a clearer vision of the limitations of these two alternatives regarding the achievement of efficient PhC laser devices.

In this paper, we report an experimental study of micrometer width photonic crystal waveguide lasers fabricated on InP substrate using the substrate approach. Unlike previous works in the same approach [3]–[5], which were mainly focused on wide ($>$1.6 μm) coupled cavities in triangular lattice PhC, the edge emitting laser structures studied here are formed by straight (W1 or W3) waveguides either in triangular or in square lattice PhCs. The lattice period varies over a very large scale, thereby allowing a detailed exploration of the behaviors of these reference waveguide lasers. In all cases, we show that the lasers can operate in a distributed-feedback (DFB) like regime with a relatively large side-mode suppression ratio at 1.55 μm. One interest of such a laterally modulated waveguide structure as compared to classical DFB structures stems from the fact that no regrowth is needed during the device fabrication. A major result in this work is the fact that most of these DFB-like structures are intrinsically single mode. The mechanism involved in mode selection is shown to be fundamentally different from the ones classically used in traditional first-order DFB lasers. By contrast, it is similar to the mode-selection previously observed in second-order DFB lasers [6], [7].

This paper is organized as follows. The fabricated PhC waveguides and the experimental setup used for their characterizations are described in Section II. Sections III and IV are devoted to the presentation and discussion of the experimental results obtained on triangular and square lattice photonic crystal waveguides, respectively. Two-dimensional plane wave calculations are used to explain the spectral behavior of the laser emission. Finally, the light-light curves and the relative thresholds of the different laser structures are compared in Section V, which is followed by a general conclusion.

II. Photonic Crystal Structures and Experimental Setup

All the PhC waveguide lasers were fabricated in an InP/InGaAsP/InP laser structure including six compressively strained InGaAsP quantum wells whose emission was centered at 1550 nm. Systematic study of the spectral behavior of the laser is allowed by the use of PhC periods ranging from 320 to 540 nm by steps of 20 nm in both triangular and square lattice PhC

Manuscript received November 17, 2004; revised June 16, 2005. This work was supported in by the French RNRT Project CRISTEL.

X. Checoury, P. Boucaud, and J.-M. Lourtioz are with the Institut, d'Électronique Fondamentale, Université Paris-Sud, 91405 Orsay Cedex, France (e-mail: Xavier.checoury@ief.u-psud.fr).

F. Pommereau, C. Cuisin, E. Derouin, O. Drisse, L. Legouezigou, O. L. Legouezigou, F. Lelarge, F. Poingt, and G.-H. Duan are with the Alcatel Thales III–V Laboratoire, Alcatel Research and Innovation, 91460 Marcoussis Cedex, France.

S. Bonnefont, D. Mulin, J. Valentin, O. Gauthier-Lafaye and F. Lozes-Dupuy are with LAAS-CNRS, 31077 Toulouse Cedex 4, France.

A. Talneau is with the Laboratoire de Photonique et Nanostructures, 91460 Marcoussis Cedex, France.

Digital Object Identifier 10.1109/JSTQE.2005.853751

structures. The air filling factor was kept to 30% and 26% for the triangular and square lattice respectively. These standard values are compatible with the etching of 4 μm deep holes through the whole semiconductor heterostructure [8]. Waveguides were fabricated in the main crystal directions for each PhC (ΓK and ΓM for the triangular lattice, and ΓX for the square lattice). Following the common terminology, W1 and W3 waveguides are associated to one and three rows of missing holes, respectively. They can be obtained in the ΓK direction of the triangular lattice as well as in the ΓX direction of the square lattice. In contrast, the so-called W2-3 waveguides [9] oriented in the ΓM direction of the triangular lattice present a periodically varying width, alternately determined by 2 and 3 missing holes. All these waveguide structures can potentially provide a DFB-like laser emission either inside or outside a PhC gap depending on whether the folding of the dispersion curve of the fundamental mode occurs inside the gap or not. For a guide oriented in the ΓK direction of the triangular lattice and a 30% air filling factor, the fundamental mode does not fold in the gap whatever the width of the guide is. For a guide oriented in the ΓM direction of this lattice (e.g., W2-3), the third folding of the fundamental mode occurs in gap. Finally, there is no gap at all in square lattice PhCs.

In our experiments, all the waveguides were about 800 PhC periods long, resulting in an overall laser length in the range from 250 to 430 μm. A cleaved facet terminates the waveguide laser at one end. A PhC mirror is used at the other end. For the sake of simplicity, this mirror had the same lattice constant, filling factor and orientation as the rest of the PhC lattice. Finally, two series of lasers were prepared: one with antireflecting (AR) coating on the cleaved facet and another one without AR coating. A 1.06-μm pulsed YAG laser was used to optically pump the PhC waveguides. The pulse duration was fixed to 15 ns, and the repetition rate to 10 kHz. A cylindrical lens was used to focus the pump beam to a $\sim$10-μm width $\sim$2-mm-long spot. A monochromator was used to spectrally resolve the laser emission at the waveguide output. All the experiments were carried out at room temperature.

III. Triangular Lattice Photonic Crystal Waveguides

A. W2-3 Waveguide in the ΓM Direction

Fig. 1 (left) shows the band diagram of the W2-3 waveguide in the ΓM orientation. This diagram is computed using a two-dimensional plane wave expansion with the supercell method. The effective index was beforehand computed to be 3.21. The air filling factor was 30% as in the experiments. The dispersion curve of the lowest order guided mode is represented in thick lines while the white area delimits the TE gap of the triangular lattice PhC.

Fig. 1 (right) shows the emission spectra measured at room temperature for two W2-3 PhC waveguide lasers (lattice constants $a = 420$ nm, leading to a $\sim$1.2 μm-wide waveguide) with and without AR coating (gray and black curves, respectively). Both PhC lasers are pumped twice above threshold. The spectra reveal the presence of two genuine DFB modes at the normalized frequencies $a/\lambda = 0.274$ and $a/\lambda = 0.276$, respectively. These modes coexist with Fabry–Perot (FP) modes in the case of the uncoated sample, the FP emission occurring around the gain maximum. As seen, the AR coating is efficient enough to avoid the FP laser emission.

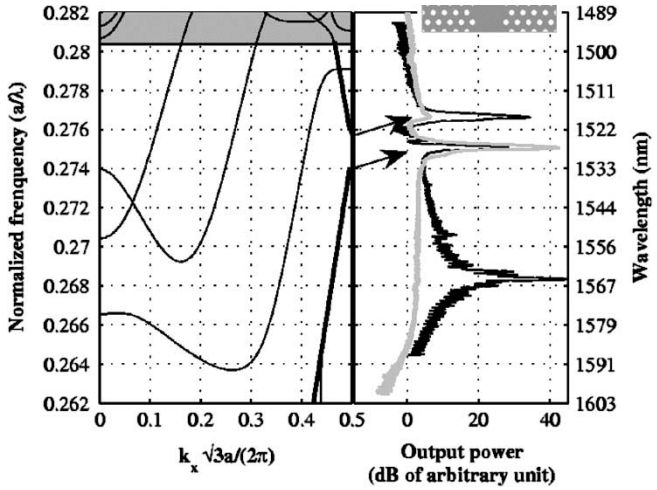

Fig. 1. Left Triangular lattice W2-3 waveguide band diagram (ΓM direction). The supercell size is 1×14 periods of the PhC lattice. The fundamental mode dispersion curve is highlighted. The white area delimits the TE gap of the triangular lattice PhC. Right: Superimposition of the emission spectra of W2-3 lasers with and without AR coating (gray and black curves, respectively) for a lattice period of 420 nm. Inset: Schematic view of the W2-3 waveguide.

It is recognized that the electromagnetic modes with a small group velocity and a high confinement in the PhC waveguide are the most favorable to produce a laser emission due to their larger interaction with the gain medium [10]. There are two such modes at the third folding of the fundamental mode dispersion curve (Fig. 1 (left), $a/\lambda = 0.275, k = \pi$/a) where a stop band appears. The calculated frequencies of the two modes defining the stop band are in agreement with the experimentally measured laser frequencies ($a/\lambda = 0.277$ and $a/\lambda = 0.275$) within a relative tolerance better than 0.5%. No other low-group-velocity mode around these normalized frequencies can yield laser emission. Therefore, we can unambiguously attribute the double-peaked laser emission to the mode pair at band edge inside the photonic band-gap. The W2-3 laser thus behaves like a third-order DFB laser. This laser is not single-mode and reveals similar losses of the two DFB components. One striking difference with a classical DFB laser is the large separation between the two DFB components. Another difference is the very low level of in-plane losses that can be expected from the existence of a complete two-dimensional photonic band gap. In contrast, out-of-plane radiation losses can never be neglected in the substrate approach.

The small discrepancy (relative error $<$0.5%) between the measured spectra and the computed band diagram may be attributed to the experimental uncertainty as well as to the overall simplification of the two-dimensional (2-D) model. A more accurate value could only be obtained with a three-dimensional (3-D) model that would take into account the InP material dispersion. Because of the good agreement between experiments and theory, no further calculations have been performed.

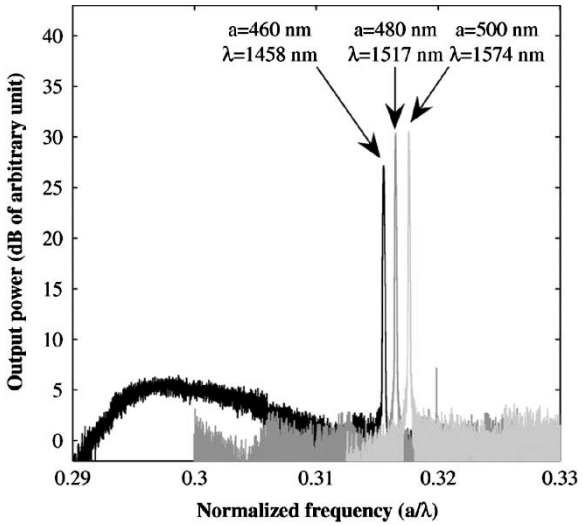

Fig. 2. Superimposition of the emission spectra of three triangular lattice W3 waveguide lasers with lattice periods of 460, 480, and 500 nm, respectively (from the darker to the lighter gray). For each laser, measurements are performed at a pump level of 1.2 times the threshold.

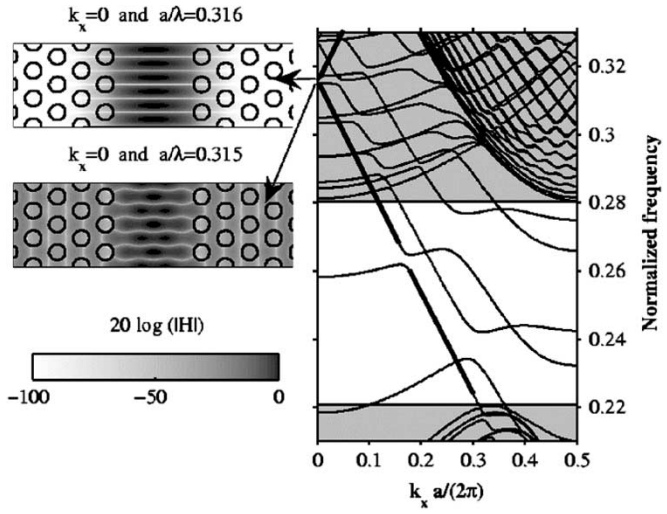

Fig. 3. Right: Band diagram calculated for a triangular lattice W3 waveguide with an air filling factor of 30% and a dielectric refractive index of 3.21. The supercell size is 1×14 periods of the PhC lattice. The fundamental mode dispersion curve is highlighted. The white area delimits the TE gap of the triangular lattice PhC. Left: H-field patterns of the fundamental W3 waveguide mode (in decibels) calculated at the frequencies of the second folding in the Brillouin zone (Γ-point).

B. W3 Waveguides in the ΓK Direction

Fig. 2 shows the superimposition of the emission spectra of three AR coated W3 lasers with PhC lattice periods equal to 460, 480, and 500 nm, respectively. The typical waveguide width is 1.4 μm. As seen in Fig. 2, all the lasers are single mode. For the 500-nm period, the laser remains single mode even at high pump powers and in the absence of AR coating. The side-mode suppression ratio can be better than 35 dB [9]. The emitted wavelength increases from 1458 to 1574 nm when the lattice period, a, is varied from 460 to 500 nm. The normalized frequency (a/λ) remains close to 0.316 and is thus almost independent of the lattice period. The very small shift from 0.3155 to 0.3176 is readily explained by the decrease of the material refractive index as the wavelength increases from 1458 to 1574 nm.

Fig. 3 shows the computed band diagram of the W3 waveguide. As seen, the frequency calculated for the second folding of the fundamental mode dispersion curve $(a/\lambda = 0.315, k = 0)$ is in good agreement with that measured for the W3 laser emission (Fig. 2). Since the W3 waveguide is designed with the same parameters as the W2-3 one, we can reasonably estimate that the discrepancy between the measured spectra and the computed band diagram is below one percent. In the frequency range of interest, only the fundamental guided mode at the Γ point has a small group velocity, and is well confined in the guide. Other small-group-velocity modes result from the coupling between a guided mode and extended modes of the crystal, which are radiating modes. Since there is no other well-confined mode calculated in the frequency range of interest, we can identify the lasing mode to the fundamental guided mode at the Γ point. In other words, the W3 laser behaves like a second-order DFB laser.

A careful inspection of the band diagram reveals indeed the opening of a narrow stopband. However, the situation is quite different from the preceding one (W2-3) where the two modes defining the mini-stopband were inside the photonic gap of the crystal. The modes considered here are outside the gap, and are thus allowed to spread over the whole crystal. Actually, plane wave calculations reveal that the 2-D H-field patterns of the two modes at the Γ point are very different (Fig. 3). The high-frequency mode represented in Fig. 3(left top) is very well confined inside the waveguide core. In contrast, the low-frequency mode (left bottom) spreads over the whole photonic crystal, and the field intensity does not decrease with the distance to the guide axis. This relative invariance of the mean field intensity with distance is observed whatever the size of the super-cell used in the computations is. Changing the size of the super-cell just leads to a small shift of the calculated frequency as well as to slight modifications of the mode pattern in the direction transverse to the guide. Actually, this mode belongs to the continuum of radiation modes similar to the ones that exist in classical refractive waveguides. The use of a finite size super-cell introduces an artificial boundary condition that imposes the frequencies of modes belonging to the continuum.

It is clearly seen from calculations that the W3 waveguide laser is intrinsically single mode thanks to the different behaviors of the two DFB-like components. The well-confined mode hardly interacts with the PhC holes, and hence only suffers low in-plane losses. The other mode spreads over the whole PhC, outside the gain region. Because of its large interaction with the PhC holes, it suffers high diffractive losses both in plane and out of plane. This situation appears to be different from that of traditional first-order DFB lasers, where the two DFB components experience similar losses. An external mechanism is needed in this case to operate the laser in single mode. This is usually achieved by breaking the translational invariance of the corrugation through the use of either a $\pi/4$ phase shift, a chirped grating or facets with different reflectivities. By contrast, the PhC W3 waveguide laser behavior is similar to that previously

reported for second-order DFB lasers [6], [7]. For second-order gratings, interference effects due to first-order diffraction of oppositely propagating guided waves have been shown to cancel the in-plane radiation loss of one of the two DFB-like components while simultaneously increasing the in-plane loss of the other component. The main differences between the present 2-D PhC laser and second-order DFB lasers stem from the use of much stronger corrugations that periodically extend in all plane directions.

C. W1 Waveguides in the ΓK Direction

Previous experiments were tentatively repeated with a triangular lattice W1 waveguide (one missing row in the ΓK direction). However, no laser emission has been observed. An inspection of the computed band diagram of this guide shows that lasing can occur at the K-point (wave vector $k = \pi$/a) corresponding to the first folding of the fundamental mode dispersion curve. The calculated frequency $(a/\lambda = 0.227)$ is both in the photonic gap and in the gain region of the quantum wells for photonic crystal periods between 340–360 nm. In the membrane approach, lasing has indeed been observed at this point [1]. However, the fact that the dispersion curve of the fundamental mode is above the light line may explain our unsuccessful attempts.

Plane wave calculations also predict that for the second folding of the fundamental mode dispersion curve $(a/\lambda = 0.332, \Gamma$ point, $k = 0)$, the W1 laser should behave like the W3 laser. Only one mode among the two modes that define the mini-stopband at this point is well confined in the guide. The other mode spreads over the whole PhC. However, the fact that W1 waveguides are twice narrower than the W3 waveguides may presently explain the absence of laser emission at the Γ point. The measured emission spectrum just revealed a bump at the corresponding frequency.

IV. Square Lattice Photonic Crystal Waveguides

In the literature, square lattice photonic crystals have been less studied than triangular lattice ones due to a smaller bandgap in TE polarization. Only a partial TE gap was predicted for the parameter values used in our PhC fabrication [i.e., for the same ratio of the hole radius to PhC period as the one used in the triangular lattice and for the same refractive index of the dielectric matrix (3.21)]. However, an absolute band gap is not mandatory to achieve a high optical confinement and single mode laser emission. Indeed, previous results on triangular lattice PhC waveguides have shown that single mode lasing is achievable outside the photonic gap. The results presented in this section confirm the existence of a similar mechanism in square lattice PhCs.

A. W3 Waveguides in the ΓX Direction

Fig. 4 shows the superimposition of the spectra emitted from two square lattice AR coated W3 waveguides with two different lattice periods (500 and 520 nm). The waveguide widths are 1.71 and 1.78 μm, respectively. A single mode laser emission is

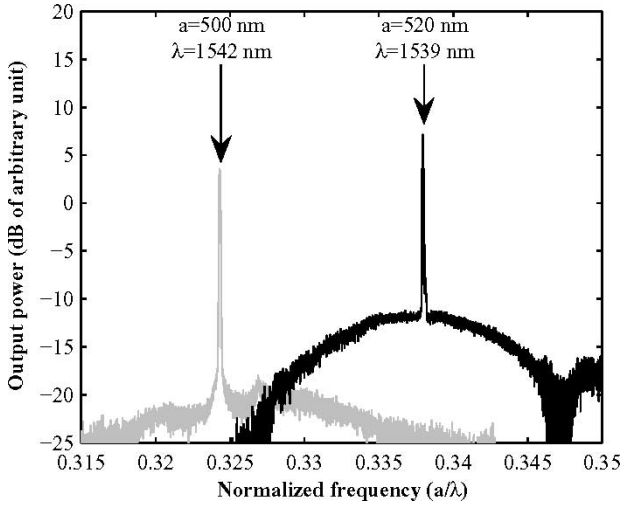

Fig. 4. Superimposition of the emission spectra of two square lattice W3 waveguide lasers with lattice periods of 500 (gray curve) and 520 nm (dark curve), respectively. For each laser, measurements are performed at a pump level of 1.2 times the threshold.

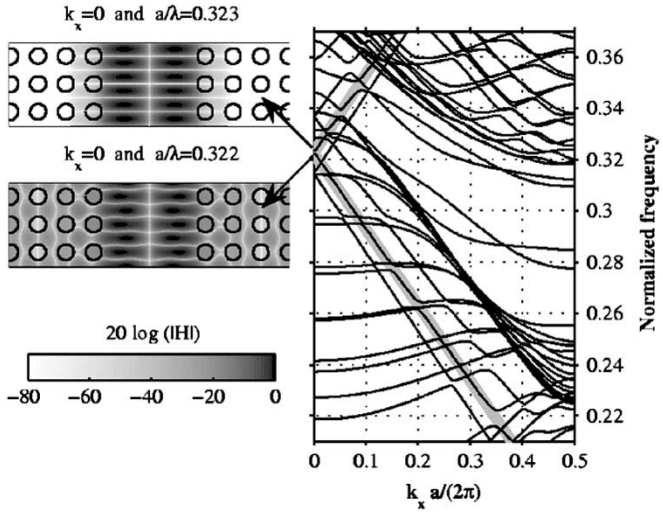

Fig. 5. Right: Band diagram calculated for a square lattice W3 waveguide with an air filling factor of 26% and a dielectric refractive index of 3.21. The supercell size is 1×16 periods of the PhC lattice. The first odd guided mode dispersion curve is highlighted. Left: H-field pattern of the first odd guided mode (in decibels) calculated at the frequencies of the second folding in the Brillouin zone (Γ-point).

obtained in both cases, but the normalized emission frequencies are different. Lasing takes place around $a/\lambda = 0.324$ and $a/\lambda = 0.338$ for the periods of 500 nm and 520 nm, respectively. Note that for the PhC period of 500 nm, the W3 laser remained single mode in the absence of AR coating. For shorter PhC periods, the emission was no longer single mode but a small isolated bump (amplified spontaneous emission) was detected in the measured spectrum near the normalized frequency $a/\lambda = 0.315$.

The band diagram of the W3 square lattice waveguide has been computed with the aim of identifying the lasing mode(s) (Fig. 5). As seen, the second folding of the fundamental mode and those of the first two higher-order modes (Γ point) occur at the normalized frequencies $a/\lambda = 0.315, 0.323$, and 0.336,

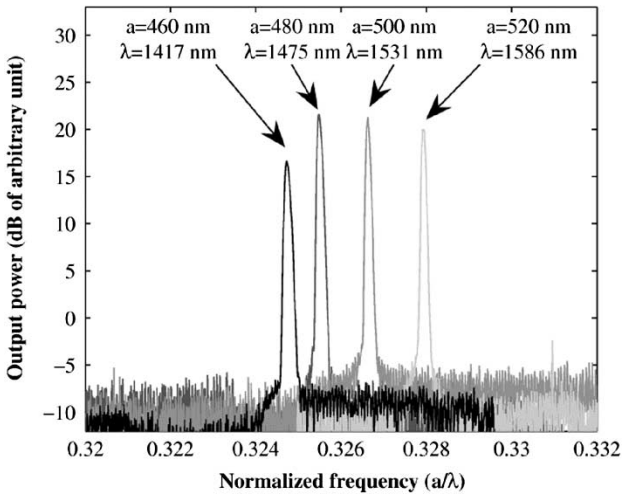

Fig. 6. Superimposition of the emission spectra of four square lattice W1 waveguide lasers with lattice periods of 460, 480, 500, and 520 nm, respectively (from the darker to the lighter gray). For each laser, measurements are performed at a pump level of 1.2 times the threshold.

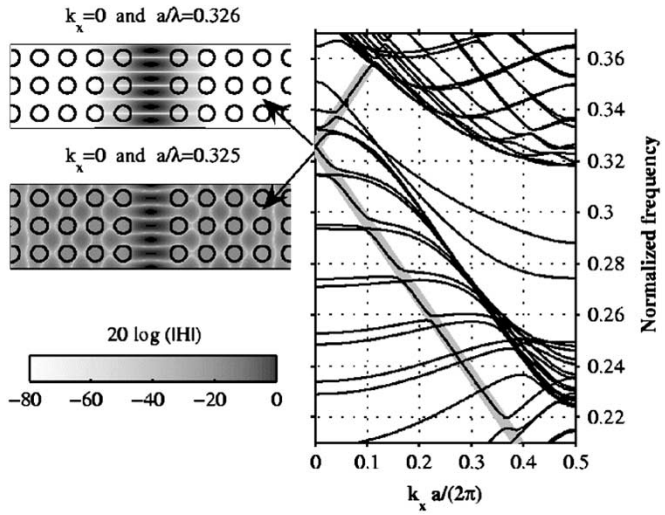

Fig. 7. Right: Band diagram calculated for a square lattice W1 waveguide with an air filling factor of 26% and a dielectric refractive index of 3.21. The supercell size is 1×14 periods of the PhC lattice. The fundamental mode dispersion curve is highlighted. Left: H-field pattern of the fundamental W1 waveguide mode (in decibels) calculated at the frequencies of the second folding in the Brillouin zone (Γ-point).

respectively. From previous considerations (Section III-A), the discrepancy between the measured and calculated frequencies is believed to be below one percent. Using the same argument as in Section III-B, the observed single mode laser emissions ($a/\lambda = 0.324$ and $a/\lambda = 0.338$) can be attributed to the second-order and third-order guided modes of the W3 waveguide, respectively. The small emission bump detected near $a/\lambda = 0.315$ should correspond to the fundamental guided mode. The reason why this mode does not lase is not clear yet.

The analysis of the band-diagram in Fig. 5 reveals the opening of narrow stopbands for the first three guided modes at the Γ point. In each case, only one of the two DFB-like components defining the stopbands is well confined in the waveguide core whereas the other one spreads over the whole photonic crystal. This is illustrated in Fig. 5 (left), which represents the H-field patterns calculated for the two DFB-like components of the second guided mode (i.e., the first odd guided mode) at the Γ-point. Actually, the situation is similar to that described in the triangular lattice W3 waveguide case. This explains why single-mode laser emissions are observed near the normalized frequencies 0.323 and 0.336 (Fig. 4).

B. W1 Waveguides in ΓX Direction

Fig. 6 shows the superimposition of four square lattice W1 waveguide laser spectra. The emission is single mode whatever the lattice period is. When the lattice period, a, varies from 460 to 520 nm, the waveguide width increases from 0.65 to 0.74 μm. The emitted wavelength is almost proportional to the lattice constant and increases from 1420 to 1580 nm. Indeed, the small shift of the normalized frequency from 0.325 to 0.328 can be attributed to the normal dispersion of the waveguide. Unlike the previous waveguide examples, the laser spectra were always exempt from Fabry–Perot oscillations around gain maximum even in the case of uncoated samples. The side mode suppression ratio was found to be greater than 25 dB whether an AR coating was used or not [11].

The band diagram of the square lattice W1 waveguide is represented in Fig. 7(right). A stopband is found at the Γ point for a normalized frequency of 0.326, which corresponds to the second folding of the fundamental mode. This calculated frequency is very close to the measured laser frequency. Again, one of the two modes defining the stopband is found to be well confined in the guide while the other one spreads over the whole crystal. This explains the single mode operation of the W1 waveguide laser.

V. Light–Light Curves

Fig. 8 shows the output powers measured for the different waveguide lasers emitting on a DFB-like modes versus the incident optical density of the pump beam. Because the pump laser is pulsed, the DFB laser linewidth is somewhat broadened (to ≈ 0.4 nm) due to transients. The output power is obtained by numerically integrating the measured spectra over $\sim$30 nm around the main emission peak(s). As seen in Fig. 8, the triangular lattice W3 and W2-3 lasers exhibit similar thresholds approximately equal to 30 kW/cm^2. This value is the peak power density really incident onto the sample. No corrections have been made for the effective power absorbed in the active medium. The square lattice W3 laser threshold is slightly lower while the square lattice W1 laser one is slightly higher. Let us notice that the threshold optical densities presently achieved per unit of laser length are of the same order of magnitude as those reported in similar pumping conditions for membrane PhC waveguide lasers [1], [2]. The waveguide width appears to have a dominant influence whether a complete TE gap is present or not. Indeed, the waveguide laser with the largest width (W3 in square lattice PhC) has the lowest threshold while the one with the narrowest width (W1 in square

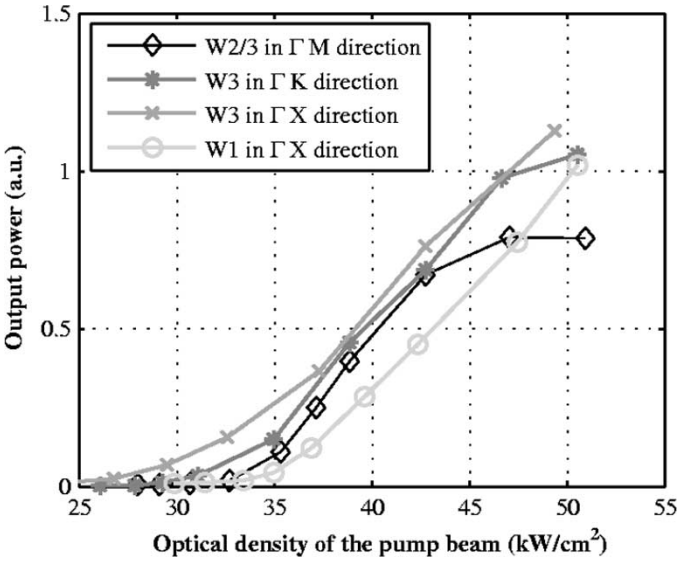

Fig. 8. Light–light characteristics of four AR coated photonic crystal waveguide lasers. From the darker to the lighter gray: W2-3 waveguide in a triangular lattice (ΓM direction, $a = 440$ nm, waveguide width $w = 1.5$ μm and waveguide length $l \sim 300$ μm), W3 waveguide in a triangular lattice (ΓK direction, $a = 500$ nm, $w = 1.45$ μm, and $l \sim 300$ μm), W3 waveguide in a square lattice (ΓX direction, $a = 520$ nm, $w = 1.7$ μm, and $l = 416$ μm) and W1 waveguide in a square lattice (ΓX direction, $a = 500$ nm, $w = 0.7$ μm, $l = 400$ μm).

lattice) has the higher threshold. Out-of-plane diffraction losses could be responsible for the higher threshold of narrow waveguide lasers. Out-of-plane diffraction losses may also critically depend on the 2-D geometry of the photonic crystal. Let us recall that the laser emission was not presently obtained from the triangular lattice W1 laser (Section III-C). Further studies are needed to clear out this point for PhC devices fabricated in the substrate approach. Nevertheless, the comparison between the W2-3 and W3 laser results indirectly suggests the interest of operating in a photonic gap. Although the W2-3 waveguide (average width $w = 1.28$ μm, length $l = 300$ μm) is narrower and shorter than the W3 waveguide ($w = 1.44$ μm, $l = 400$ μm), the two waveguide lasers have similar thresholds. Lower in-plane losses likely compensate for higher out-of plane diffraction losses.

VI. Conclusion

Lasing of canonical photonic crystal waveguides consisting of one to three defect-lines in either square or triangular lattices has been explored in the substrate approach on InP. The optical pumping technique was used. A laser emission has been obtained in all cases except for the triangular lattice W1 waveguide. We have shown that narrow PhC waveguide lasers can behave like DFB lasers whether the emission takes place inside the photonic gap (triangular lattice W2-3), above the gap (triangular lattice W3) or in the absence of complete TE bandgap (square lattice PhC W1 and W3). Contrary to what one might expect, the in-gap situation does not presently lead to the lowest threshold. Out-of-plane losses partly cancel out the benefit of a complete TE photonic bandgap, and an optimization of the W2-3 PhC waveguide geometry seems necessary for reducing the losses. In the out-of-gap cases, a single-mode DFB-like laser emission has been achieved at the Γ-point in both triangular and square lattice PhC waveguides. Calculations from a two-dimensional plane wave model have shown that only one of the two DFB-like modes is strongly confined in the guide while the other spreads over the whole crystal. To our knowledge, the square lattice W1 laser is the narrowest PhC waveguide laser which has been operated in single mode using the substrate approach. The results presented in this paper provide guidelines for the design of electrically pumped all PhC edge emitting lasers.

References

[1] A. Sugitatsu and S. Noda, "Room temperature operation of 2D photonic crystal slab defect-waveguide laser with optical pump," *Electron. Lett.*, vol. 39, no. 2, pp. 213–215, 2003.

[2] Y. Sugimoto, K. Inoue, N. Ikeda, S. Ohkouchi, Y. Tanaka, Y. Nakamura, H. Nakamura, H. Sasaki, K. Ishida, and K. Asakawa, "Room temperature operation of InAs-quantum-dot laser utilizing GaAS-photonic-crystal-slab based line defect waveguide with optical pump," in *Proc. IEEE 19th Int. Semiconductor Laser Conf.*, Matsue-shi, Japan, 2004, pp. 81–82.

[3] T. D. Happ, M. Kamp, A. Forchel, J. L. Gentner, and L. Goldstein, "Two-dimensional photonic crystal coupled-defect laser diode," *Appl. Phys. Lett.*, vol. 82, no. 1, pp. 4–6, 2003.

[4] S. Mahnkopf, M. Arlt, M. Kamp, V. Colson, D. Guang Hua, and A. Forchel, "Two-channel tunable laser diode based on photonic crystals," *IEEE Photon. Technol. Lett.*, vol. 16, no. 2, pp. 353–355, Feb. 2004.

[5] A. Talneau, L. LeGratiet, J. L. Gentner, A. Berrier, M. Mulot, S. Anand, and S. Olivier, "High external efficiency in a monomode full-photonic-crystal laser under continuous wave electrical injection," *Appl. Phys. Lett.*, vol. 85, no. 11, pp. 1913–1915, 2004.

[6] C. H. Henry, R. F. Kazarinov, R. A. Logan, and R. Yen, "Observation of destructive interference in the radiation loss of second-order distributed feedback lasers," *IEEE J. Quantum Electron.*, vol. QE-21, no. 2, pp. 151–153, Feb. 1985.

[7] R. F. Kazarinov and C. H. Henry, "Second-order distributed feedback lasers with mode selection provided by first-order radiation losses," *IEEE J. Quantum Electron.*, vol. QE-21, no. 2, pp. 144–150, Feb. 1985.

[8] F. Pommereau, L. Legouezigou, S. Hubert, S. Sainson, J. P. Chandouineau, S. Fabre, G. H. Duan, B. Lombardet, R. Ferrini, and R. Houdre, "Fabrication of low loss two-dimensional InP photonic crystals by inductively coupled plasma etching," *J. Appl. Phys.*, vol. 95, no. 5, pp. 2242–2245, 2004.

[9] X. Checoury, P. Boucaud, J.-M. Lourtioz, F. Pommereau, C. Cuisin, E. Derouin, O. Drisse, L. Legouezigou, F. Lelarge, F. Poingt, G. H. Duan, D. Mulin, S. Bonnefont, O. Gauthier-Lafaye, J. Valentin, F. Lozes, and A. Talneau, "Distributed feedback regime of photonic crystal waveguide lasers at 1.5 μm," *Appl. Phys. Lett.*, vol. 85, no. 23, pp. 5502–5504, 2004.

[10] K. Sakoda, *Optical Properties of Photonic Crystals*. Berlin, Heidelberg: Springer-Verlag, 2001.

[11] X. Checoury, P. Boucaud, J.-M. Lourtioz, F. Pommereau, C. Cuisin, E. Derouin, O. Drisse, L. Legouezigou, F. Lelarge, F. Poingt, G. H. Duan, D. Mulin, S. Bonnefont, J. Valentin, F. Lozes, and A. Talneau, "Square lattice photonic crystal waveguides for lasers emitting at 1.55 μm," in *Proc. IEEE 19th Int. Semiconductor Laser Conf.*, Matsue-shi, Japan, 2004, pp. 131–132.

Xavier Checoury was born in Boulogne-Billancourt, France, in 1974. He received the M.S. degree from the Ecole Nationale Supérieure des Télécommunications, Paris, France, in 1998. He is currently working towards the Ph.D. degree at the Institut d'Electronique Fondamentale (IEF), University of Paris-Sud.

From 1999 to 2002, he was an R&D Engineer on radio-frequency emitters at EADS Telecom, Paris. His research interest concerns photonic crystals, semiconductor lasers, and numerical modeling.

Philippe Boucaud received the M.S. degree in solid-state physics and the Ph.D. degree in optical nonlinearities in semiconductor quantum well from the University of Paris XI, Paris, France, in 1987 and 1992, respectively.

Since 1993, he has been a Permanent Researcher at the French National Center of Scientific Research (CNRS). He is currently working at Institut

d'Electronique Fondamentale (IEF), University of Paris-Sud, France, which he joined in 1988. He was a Postdoctoral Fellow at France Telecom CNET in 1992, where he worked on the growth and optical properties of SiGeC heterostructures. He was a Visiting Researcher at the University of California at Santa Barbara during 1999. His current research focuses on self-assembled quantum nanostructures for quantum information and the development photonic devices with Ge/Si self-assembled islands. He has been Head of the Nanophotonic and Ultrafast Electronics Research group at IEF since 2001. He has coauthored over 130 articles in the field of semiconductor heterostructures.

Jean-Michel Lourtioz was born in Lens, France, in 1948. He graduated from Ecole Centrale de Paris, France, in 1971, and received the equivalent of the M.S. degree in physics and the Ph.D. degree from the University of Paris, in 1975 and 1981, respectively.

Since 1976, he has been with CNRS, and has worked at the Institut d'Electronique Fondamentale (IEF), University of Paris-Sud, France. He is presently Directeur de Recherche at CNRS and is the head of IEF. From 1996 to 2001, he coordinated the research studies on photonic crystals and microcavities. Since 2002, he has coordinated the French network on nanophotonics. His current research interests include optical and electronic devices, semiconductor nanostructures, photonic crystals, and microcavities.

Frédéric Pommereau received the Doctorate degree from the Université de Paris XI, Orsay, France, in 1989. His Ph.D. dissertation is on the modeling of contact lithography for the fabrication of GaAs ICs.

From 1989 to 1991, he was engaged in the fabrication of integrated circuits on silicon with MATRA MHS. He joined Alcatel Alsthom Research Marcoussis, France, in 1991, and has been involved in research activities on semiconductor optical amplifiers (SOA), arrayed waveguides and SOAs, high-speed photodiodes, and more recently, photonic crystals. He is now responsible within Alcatel Thales III–V Laboratoire for technology implementation including lithography and etching on III–V semiconductors, and is involved in several European projects and French national RNRT projects.

C. Cuisin, photograph and biography not available at the time of publication.

E. Derouin, photograph and biography not available at the time of publication.

O. Drisse, photograph and biography not available at the time of publication.

L. Legouezigou, photograph and biography not available at the time of publication.

O. L. Legouezigou, photograph and biography not available at the time of publication.

François Lelarge was born in France, in 1966. He received the Diploma in material science and the Ph.D. degree from the University of Pierre et Marie Curie, Paris, France, in 1993, and 1996 respectively.

From 1993 to 1996, he was with the Laboratory of Microstructures and Microelectronic, CNRS Bagneux, France. His thesis work was devoted to the fabrication and the optical characterization of GaAs/AlAs lateral supperlattice grown on vicinal surfaces by MBE. From 1997 to 2000, he was a Postdoctoral Researcher at the Institute of Micro and Optoelectronics, Lausanne, Switzerland. He worked on InGaAs/GaAs quantum wires fabrication by MOCVD regrowth on patterned substrates. Presently, he is working within Alcatel Thales III–V Laboratoire on InGaAsP/InP GSMBE growth for optoelectronic devices, Palaiseau, France.

F. Poingt, photograph and biography not available at the time of publication.

Guang-Hua Duan (S'88–M'90–SM'01) was born in Hubei Province, China, on January 23, 1964. He received the B.E. degree from Xidian University, Xi'an, China, in 1983 and the M.E. and Doctorate degrees from the Ecole Nationale Supérieure des Télécommunications (ENST), France, in 1987 and 1991, respectively, all in applied physics. He was habilitated to direct researches by Université de Paris-Sud in 1995.

From 1991 to 1992, he was a Postdoctoral Fellow supported by both Alcatel Alsthom Research and ENST. From 1992 to 2000, he was an Assistant, then an Associate Professor at ENST. From 1998 to 1999, he was with the University of Maryland as a Visiting Associate Professor. He joined Opto+, Alcatel Research and Innovation Center in Marcoussis on October 2000. He is now the leader of the team "advanced photonic components" within Alcatel Thales III–V Laboratoire, with research activities on photonic crystals, advanced semiconductor lasers and functional optoelectronic sub-systems for core and metro networks. He is author or coauthor of more than 100 research papers, eight patents and a contributor to the book *Semiconductor Lasers: Past, Present, and Future* (New York: AIP, 1995). He lectures in the fields of electromagnetism, optoelectronics and laser physics in ENST and in Ecole Supérieure d'Optique.

S. Bonnefont, photograph and biography not available at the time of publication.

D. Mulin, photograph and biography not available at the time of publication.

J. Valentin, photograph and biography not available at the time of publication.

O. Gauthier-Lafaye, photograph and biography not available at the time of publication.

F. Lozes-Dupuy, photograph and biography not available at the time of publication.

A. Talneau, photograph and biography not available at the time of publication.